

Discovering the top partners at the LHC using same-sign dilepton final states

Roberto Contino^a and G eraldine Servant^{a,b}

^a *CERN Physics Department, Theory Division, CH-1211 Geneva 23, Switzerland*

^b *Service de Physique Th eorique, CEA Saclay, F91191 Gif-sur-Yvette, France*

roberto.contino@cern.ch, geraldine.servant@cern.ch

Abstract

A natural, non-supersymmetric solution to the hierarchy problem generically requires fermionic partners of the top quark with masses not much heavier than 500 GeV. We study the pair production and detection at the LHC of the top partners with electric charge $Q_e = 5/3$ ($T_{5/3}$) and $Q_e = -1/3$ (B), that are predicted in models where the Higgs is a pseudo-Goldstone boson. The exotic $T_{5/3}$ fermion, in particular, is the distinct prediction of a LR custodial parity invariance of the electroweak symmetry breaking sector. Both kinds of new fermions decay to Wt , leading to a $t\bar{t}WW$ final state. We focus on the golden channel with two same-sign leptons, and show that a discovery could come with less than 100 pb^{-1} (less than 20 fb^{-1}) of integrated luminosity for masses $M = 500\text{ GeV}$ ($M = 1\text{ TeV}$). In the case of the $T_{5/3}$, we present a simple strategy for its reconstruction in the fully hadronic decay chain. Although no full mass reconstruction is possible for the B , we still find that the same-sign dilepton channel offers the best chances of discovery compared to other previous searches that used final states with one or two opposite-sign leptons, and hence suffered from the large $t\bar{t}$ background. Our analysis also directly applies to the search of 4th generation b' quarks.

1 Introduction

If one looks at the formidable legacy left by the LEP experiments, probably the most precious clue to unravel the mystery on the nature of the Electroweak Symmetry Breaking (EWSB) is the evidence, although not yet conclusive, in favor of a light Higgs [1]. According to the modern understanding of field theories, combined with an intuitive naturalness criterion, the existence of a light scalar in the low-energy spectrum, such as a light Higgs boson, is a clear indication of a highly non-trivial completion of the Standard Model (SM), with a new symmetry and new particles. Or, it might be the sign of a dramatic failure of naturalness arguments [2–4].

The most notorious example of symmetry protection for the light Higgs is Supersymmetry: according to its paradigm, the radiative correction of each SM field to the Higgs mass is fine tuned against that of a superpartner of opposite statistics. The top quark contribution, in particular, is balanced by the contribution of its scalar partners, the stops. Another kind of symmetry protection, however, could be at work: the light Higgs could be the pseudo-Goldstone boson of a spontaneously broken global symmetry [5–7]. In this case the radiative correction of the top quark to the Higgs mass is balanced by the contribution of new partners of the same spin. The naturalness criterium suggests that these new heavy fermions should have masses below, or not much heavier than, 1 TeV. It is the production of these top partners at the LHC that we want to study in this paper.

Particularly motivated is the possibility that the spontaneous breaking of the global symmetry and the new states originate from a strongly-coupled dynamics. This would allow for a complete resolution of the Hierarchy Problem without the need of fundamental scalar fields, and would make it possible to generate a large enough quartic coupling for the Higgs via radiative effects. As suggested by the theoretical developments on the connection between gravity in higher-dimensional curved spacetimes and strongly-coupled gauge theories [8, 9], the strong dynamics that generates the light Higgs could be realized by the bulk of an extra dimension [10]. These extra-dimensional theories are not only fascinating because of the profound impact they would have on our understanding of high-energy physics, but are also extremely interesting as they admit, under certain assumptions, a perturbative expansion that allows one to compute several observables of key interest, such as for example the Higgs potential.

The LEP precision data are once again crucial in guiding our theoretical investigation, as they seem to be compatible only with a specific kind of strong dynamics: the new sector must possess a custodial symmetry $G_C = \text{SU}(2)_C$ to avoid large tree-level corrections to the ρ parameter [11]. This in turn implies an unbroken $\text{SU}(2)_L \times \text{SU}(2)_R \times \text{U}(1)_X$ invariance of the strong dynamics before EWSB, meaning that its resonances, in particular the heavy partners of the top quark, will fill multiplets of such symmetry. It has been recently pointed out [12] that possible modifications to the $Z\bar{b}_L b_L$ coupling can also be substantially suppressed, and the relative LEP constraint more easily satisfied, if the custodial symmetry of the strong sector includes a LR parity, $G_C = \text{SU}(2)_C \times P_{LR}$. More precisely, the $Z\bar{b}_L b_L$ vertex will not receive zero-momentum corrections from the strong dynamics if b_L couples linearly to a composite fermionic operator transforming as a $(\mathbf{2}, \mathbf{2})_{2/3}$ under $\text{SU}(2)_L \times \text{SU}(2)_R \times \text{U}(1)_X$ (hypercharge being defined as $Y = T_R^3 + X$). In this case, as explicitly illustrated by the 5-dimensional models built to incorporate the P_{LR} protection [13–16], the heavy partners

of (t_L, b_L) can themselves fill a $(\mathbf{2}, \mathbf{2})_{2/3}$ representation. The latter consists of two $SU(2)_L$ doublets: the first, (T, B) , has the quantum numbers of (t_L, b_L) ; the second – its “custodian” – is made of one fermion with exotic electric charge $Q_e = +5/3$, $T_{5/3}$, and one with charge $Q_e = +2/3$, $T_{2/3}$. Since the Higgs transforms like a $(\mathbf{2}, \mathbf{2})_0$, the partners of t_R , if any, will form a $(\mathbf{1}, \mathbf{1})_{2/3}$ or a $[(\mathbf{1}, \mathbf{3}) \oplus (\mathbf{3}, \mathbf{1})]_{2/3}$ of $SU(2)_L \times SU(2)_R \times U(1)_X$ [12].

As explained in detail in Section 2, these new fermions are expected to couple strongly to the third generation SM quarks plus one longitudinal W , Z gauge boson or the Higgs. These interactions are responsible for both their single production in hadron collisions and their decay, while pair production will proceed via QCD interactions. The production at the LHC of the heavy fermions with electric charge $+2/3$ (the heavy tops \tilde{T} , T , $T_{2/3}$) has been studied in detail in the literature, mainly because of their role in Little Higgs models. Pair production of the $SU(2)_L$ singlet \tilde{T} , $gg, q\bar{q} \rightarrow \tilde{T}\tilde{T}^*$, was considered in [17], focussing on final states with one charged lepton. The process with both heavy tops decaying to Wb was found to be the most promising, though channels with one neutral decay to Z or h help increase the discovery reach as well. The minimum integrated luminosity to have a 5σ statistical significance, $\mathcal{S}/\sqrt{\mathcal{B}} = 5$, was found to be $L_{min}(5\sigma) = 2.1 \text{ fb}^{-1}$ (90 fb^{-1}) in the case of a heavy top with mass $M_{\tilde{T}} = 500 \text{ GeV}$ (1 TeV). As found in Ref. [18], the significance is enhanced if the $\tilde{T}\tilde{T}^*$ pair-production cross section receives an additional contribution from the exchange of a heavy gluon. Single production via bW fusion, $qb \rightarrow q'\tilde{T}$, was considered in Refs. [19], focussing on leptonic final states. It was found to extend the discovery reach to $M_{\tilde{T}} = 2$ (2.5) TeV, for $L = 300 \text{ fb}^{-1}$ and a value of the $\tilde{T}bW$ coupling equal to $\lambda_{\tilde{T}} = 1$ (2).

Pair production of the heavy fermion with electric charge $-1/3$ (the heavy bottom B) has also been recently considered in [20, 21].¹ The process $gg, q\bar{q} \rightarrow B\bar{B} \rightarrow W^-tW^+\bar{t}$ leads to spectacular events with $4W$ ’s and two bottom quarks, though its observability into final states with one charged lepton or two leptons with opposite charge is challenged by the large $t\bar{t} + jets$ SM background. To get rid of the latter, Refs. [20] and [21] performed hard cuts on the total effective mass respectively of the jets and of the entire event. Ref. [21] also proposed the use of the single-jet invariant mass distribution as a strategy to further isolate the signal events and reconstruct the hadronically decayed B . The basic idea is that the top and the W originating from the decay of a very massive B are highly boosted, and the quarks emitted in their hadronic decay will merge into a single jet with invariant mass M_j close to m_W or m_t .

In this paper we want to study the pair production of the B and of its custodial partner $T_{5/3}$ proposing a different strategy to get rid of the $t\bar{t} + jets$ background: looking at final states with two *same-sign* leptons. Once pair produced, both the heavy bottom B and the exotic $T_{5/3}$ decay to $W^+W^+W^-W^-b\bar{b}$, although with different spatial configurations as dictated by their different electric charges, see Fig. 1. In the case of the $T_{5/3}$ the two same-sign leptons come from the decay of the same heavy fermion, allowing for a full reconstruction of the hadronically-decaying $T_{5/3}$, while in the case of the heavy bottom they come from different B ’s. Despite the fact that a full reconstruction of the B is not possible, we still find that the same-sign dilepton channel is probably the most promising one for its discovery.

In the next section we present a simple effective lagrangian for the top partners valid at low energy. We then describe our Monte Carlo simulation (section 3), and define our strategy

¹See also [22] for an earlier study.

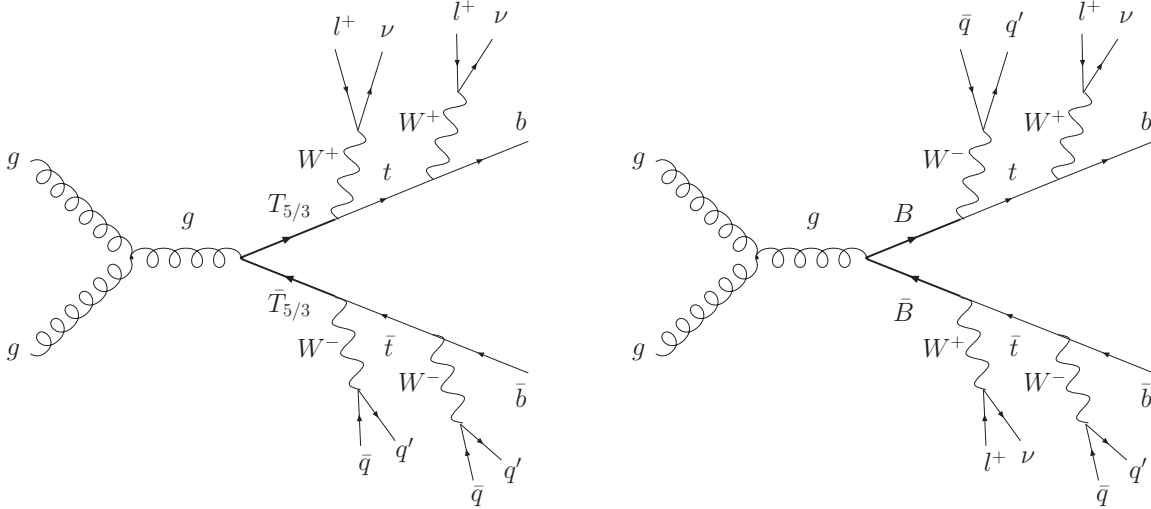


Figure 1: Pair production of $T_{5/3}$ and B to same-sign dilepton final states.

(section 4). Sections 5 and 6 present our main analysis: first, we show the optimal cuts and characterize the best observables for discovering the heavy $T_{5/3}$ and B without making any sophisticated reconstruction; then, we reconstruct the W and t candidates and pair them to reconstruct the $T_{5/3}$ invariant mass. We conclude with a critical discussion of our results.

2 A simple model for the top partners

Although the main results of our analysis will be largely independent of the specific realization of the new sector, we will adopt as a working example the “two-site” description of Ref. [23], which reproduces the low-energy regime of the 5D models of [13, 14] (see also [24] for an alternative 4D construction). Its two building blocks are the weakly-coupled sector of the elementary fields $q_L = (t_L, b_L)$ and t_R , and a composite sector comprising two heavy multiplets $(\mathbf{2}, \mathbf{2})_{2/3}$, $(\mathbf{1}, \mathbf{1})_{2/3}$ plus the Higgs (the case with partners of the t_R in a $[(\mathbf{1}, \mathbf{3}) \oplus (\mathbf{3}, \mathbf{1})]_{2/3}$ can be similarly worked out):

$$\mathcal{Q} = (\mathbf{2}, \mathbf{2})_{2/3} = \begin{bmatrix} T \\ B \end{bmatrix}, \quad \tilde{T} = (\mathbf{1}, \mathbf{1})_{2/3}, \quad \mathcal{H} = (\mathbf{2}, \mathbf{2})_0 = \begin{bmatrix} \phi_0^+ & \phi^+ \\ -\phi^- & \phi_0 \end{bmatrix}. \quad (1)$$

The two sectors are linearly coupled through mass mixing terms, resulting in SM and heavy mass eigenstates that are admixtures of elementary and composite modes. The Higgs doublet couples only to the composite fermions, and its Yukawa interactions to the SM and heavy eigenstates arise only via their composite component. The Lagrangian in the elementary/composite basis is (we omit the Higgs potential and kinetic terms and we assume, for simplicity, the same Yukawa coupling for both left and right composite chiralities):

$$\begin{aligned} \mathcal{L} = & \bar{q}_L \not{\partial} q_L + \bar{t}_R \not{\partial} t_R \\ & + \text{Tr} \{ \bar{\mathcal{Q}} (\not{\partial} - M_Q) \mathcal{Q} \} + \bar{\tilde{T}} (\not{\partial} - M_{\tilde{T}}) \tilde{T} + Y_* \text{Tr} \{ \bar{\mathcal{Q}} \mathcal{H} \} \tilde{T} + h.c. \\ & + \Delta_L \bar{q}_L (T, B) + \Delta_R \bar{t}_R \tilde{T} + h.c. \end{aligned} \quad (2)$$

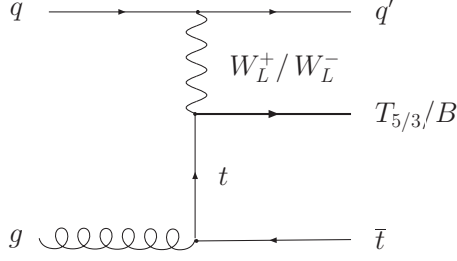


Figure 2: Associated single production of B and $T_{5/3}$ at the LHC.

where M_Q , $M_{\tilde{T}}$ are the masses of the composite states, Y_* their Yukawa coupling and Δ_L , Δ_R are the mixing masses between elementary and composite fields. After rotating to the mass eigenstate basis, the Yukawa Lagrangian reads (now denoting with q_L , t_R the SM fields, and with T , B , $T_{5/3}$, $T_{2/3}$, \tilde{T} the heavy mass eigenstates):

$$\begin{aligned} \mathcal{L}_{yuk} = & Y_* \sin \varphi_L \sin \varphi_R \left(\bar{t}_L \phi_0^\dagger t_R - \bar{b}_L \phi^- t_R \right) + Y_* \cos \varphi_L \sin \varphi_R \left(\bar{T} \phi_0^\dagger t_R - \bar{B} \phi^- t_R \right) \\ & + Y_* \sin \varphi_L \cos \varphi_R \left(\bar{t}_L \phi_0^\dagger \tilde{T} - \bar{b}_L \phi^- \tilde{T} \right) + Y_* \sin \varphi_R \left(\bar{T}_{5/3} \phi^+ t_R + \bar{T}_{2/3} \phi_0 t_R \right) + \dots \end{aligned} \quad (3)$$

Here the dots stand for terms with two heavy fermions, and $\sin \varphi_{L,R}$ denote the degree of compositeness of the SM $t_{L,R}$ quarks: $\tan \varphi_L = \Delta_L / M_Q$, $\tan \varphi_R = \Delta_R / M_{\tilde{T}}$ [23]. Equation (3) explicitly illustrates the specific pattern expected for the couplings of the heavy fermions: they couple to one (third-generation) SM quark of defined chirality plus one longitudinal W or Z boson, or the Higgs. The values of the couplings are linked to the SM top Yukawa coupling y_t ; in the two-site model, in particular, the largest couplings are to the SM fermions with the largest composite component. For example, if $1 < Y_* \ll 4\pi$ – as one naturally expects if the heavy fermions are bound states of a strongly coupled sector – the couplings of T , B , $T_{5/3}$, $T_{2/3}$ are large in the limit of t_R mainly composite, $Y_* \cos \varphi_L \sin \varphi_R \simeq Y_* \sin \varphi_R \gg y_t$, while those of \tilde{T} are suppressed [23]. Also, the small ratio between the bottom and top quark masses can be easily explained in this scheme by assuming that the b_R has a very small composite component. This in turn implies that any coupling of b_R to the heavy fermions will be suppressed (for that reason we have omitted b_R and its own partner(s) from the Lagrangian (2)). Finally, notice that the presence of flavour-changing neutral interactions distinguishes the heavy partners T , B from a fourth generation.

As anticipated, the interactions of eq.(3) are responsible for both the decay and the single production of the heavy fermions (see for example Ref. [23] for a more detailed discussion). Pair production will instead proceed via QCD interactions. In this work we focus on the pair production of B and $T_{5/3}$ at the LHC, considering two values of their mass: $M = 500$ GeV and $M = 1$ TeV. Both $T_{5/3}$ and B decay exclusively to one top plus one longitudinally polarized W , with a decay width

$$\Gamma(T_{5/3}/B \rightarrow t_R W_L) = \frac{\lambda^2}{32\pi} M \left[\left(1 + \frac{m_t^2 - m_W^2}{M^2} \right) \left(1 + \frac{m_t^2 + 2m_W^2}{M^2} \right) - 4 \frac{m_t^2}{M^2} \right] \times \zeta^{1/2}, \quad (4)$$

where

$$\zeta \equiv 1 - 2 \frac{m_t^2 + m_W^2}{M^2} + \frac{(m_t^2 - m_W^2)^2}{M^4}, \quad (5)$$

and $M = M_{T_{5/3}}$ ($M = M_B$), $\lambda = \lambda_{T_{5/3}} = Y_* \sin \varphi_R$ ($\lambda = \lambda_B = Y_* \cos \varphi_L \sin \varphi_R$) in the case of $T_{5/3}$ (B). For example, setting $\lambda = 3$ gives $\Gamma = 31$ (82) GeV for $M = 0.5$ (1) TeV. Single production proceeds via the diagram of Fig. 2, and becomes dominant for heavier masses, see Fig. 3.² For simplicity, although it is likely to be important for extending the discovery reach to larger masses, we will neglect single production in the present work. We will argue that this should not affect significantly our final results, and that it is in fact a conservative assumption.

Finally, it is worth mentioning that no direct bounds on the heavy quark masses $M_{T_{5/3}}$, M_B exist from Tevatron, as no searches have been pursued for new heavy quarks decaying to tW . The CDF bound on heavy bottom quarks b' , $M_{b'} > 268$ GeV, is derived assuming that b' decays exclusively to bZ [25]. We estimate that for $M = 300$ GeV (500 GeV), the pair-production cross section of $T_{5/3}$ or B at Tevatron is 201 fb (1 fb). For $M = 300$ GeV this corresponds to ~ 35 events in the same-sign dilepton channel, before any cut, with an integrated luminosity of 4 fb^{-1} , suggesting that, although challenging, a dedicated analysis at CDF and D0 could lead to interesting bounds on $M_{T_{5/3}}$, M_B .³

3 Signal and Background Simulation

We want to study the pair production of B and $T_{5/3}$ at the LHC focussing on decay channels with two same-sign leptons. We consider two values of the heavy fermion masses, $M = 500$ GeV and $M = 1$ TeV, and set $\lambda_{T_{5/3}} = \lambda_B = 3$. As explained in the previous section, such large values of the couplings are naturally expected if the heavy fermions are bound states of a strongly coupled sector, and t_R is mainly composite.⁴ Notice, however, that our final results will be largely independent of the specific values of $\lambda_{T_{5/3}}$, λ_B , since the latter determine only the decay width of the heavy fermions. For our choice of couplings $\Gamma = 31$ (82) GeV for $M = 0.5$ (1) TeV.

At the hard-scattering level, the process responsible for pair production to two same-sign leptons is:

$$gg, q\bar{q} \rightarrow B\bar{B}, T_{5/3}\bar{T}_{5/3} \rightarrow l^\pm \nu l^\pm \nu b\bar{b} q\bar{q}' q\bar{q}'. \quad (6)$$

The physical, observed final state is of the form

$$pp \rightarrow l^\pm l^\pm + n \text{ jets} + \cancel{E}_T, \quad l = e, \mu, \quad (7)$$

²Notice that the exact expression for the coupling $\lambda_{T_{5/3}}$ is given by $\lambda_{T_{5/3}} = (M_{T_{5/3}}/m_W)(g/\sqrt{2})\sin\theta$, where $\sin\theta$ parametrizes the composite $T_{2/3}$ component of the SM t_R eigenstate after EWSB, which can be derived by diagonalizing the 4×4 mass matrix of charge $2/3$ fermions. Here we approximate the exact value of $\sin\theta$ at first order in a power series of electroweak insertions, which gives $\sin\theta \simeq vY_* \sin\varphi_R/\sqrt{2}M_{T_{5/3}}$ for $\sin\theta \ll 1$. A similar expression can be derived for λ_B . This approximation breaks down for large values of Y_* and light masses M , so that $O(1)$ corrections to the value of the single production cross section in Fig. 3 are expected for $M \lesssim 500$ GeV and $\lambda \sim 3 - 4$. We thank J. A. Aguilar-Savedra for pointing this out. For example, for $M_{T_{5/3}} = 500$ GeV, $Y_* = 4$, $\sin\varphi_R = 0.75$, $\sin\varphi_L = 0.58$, the exact diagonalization gives $\sin\theta = 0.69$, to be compared with the perturbative value $(vY_* \sin\varphi_R/\sqrt{2}M_{T_{5/3}}) = 1.04$. Even $O(1)$ corrections to the $T_{5/3}$ and B decay widths, which are difficult to extract anyway due to the finite jet energy resolution, do not affect our analysis.

³An inclusive search for new physics with same-sign dilepton events was performed recently by CDF using 1 fb^{-1} of data [26], although these results were not translated into bounds on B and $T_{5/3}$ masses. It will be interesting to see whether the observed slight excess of events persists when using larger data sets.

⁴For example, $\lambda_{T_{5/3}}, \lambda_B \simeq 3$ for $Y_* = 3$ and $\sin\varphi_R, \cos\varphi_L \simeq 1$, see eq.(3).

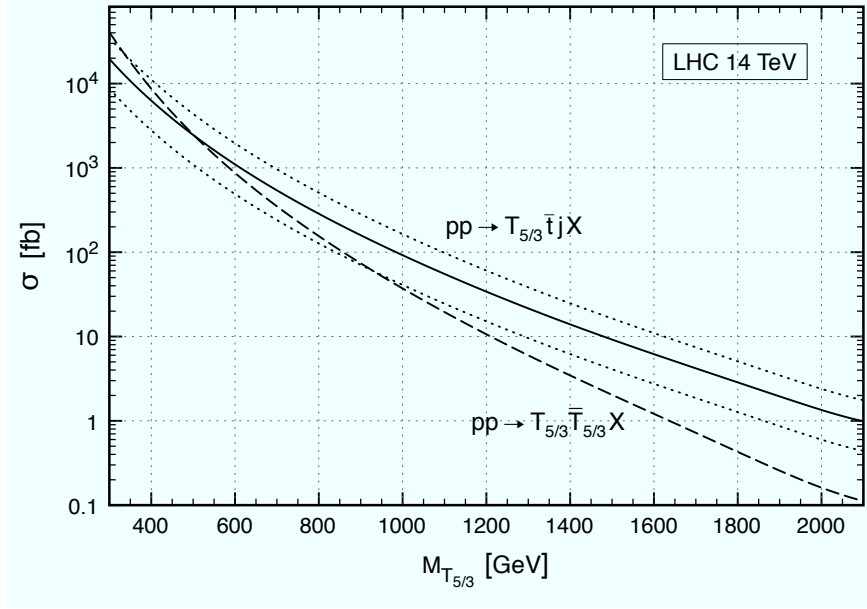


Figure 3: Production cross sections at the LHC for $T_{5/3}$ as functions of its mass. The dashed line refers to pair-production; the solid and the two dotted curves refer to single production for the three values of the coupling (from highest to lowest) $\lambda_{T_{5/3}} = Y_* \sin \varphi_R = 4, 3, 2$. Cross sections for B are given by the same curves for the same values of $\lambda_B = Y_* \cos \varphi_L \sin \varphi_R$.

where the number of jets depends on the adopted jet algorithm and on its parameters. In our analysis we will require $n \geq 5$; this choice will be motivated by the distributions and the considerations presented in the next section. The most important SM backgrounds to the process of eq.(7) are $t\bar{t}W + jets$, $t\bar{t}WW + jets$ (including the $t\bar{t}h + jets$ resonant contribution for $m_h \geq 2m_W$), $WWW + jets$ (including the $Wh + jets$ resonant contribution for $m_h \geq 2m_W$), $W^\pm W^\pm + jets$ and $Wl^+l^- + jets$ (including the $WZ + jets$ contribution) where one lepton is missed. To be conservative and consider the case in which the background is largest, we have set the Higgs mass to $m_h = 180$ GeV. This greatly enhances the $t\bar{t}WW$ and WWW backgrounds.

We have generated both the signal and the SM background events at the partonic level with MadGraph/MadEvent [27],⁵ and we have used Pythia [28] for showering and to include the initial and final-state radiation (for simplicity, hadronization and underlying event have been switched off in Pythia). Jets have been reconstructed using F. Paige's GETJET cone algorithm with $E_T^{min} = 30$ GeV and two different values of the cone size $\Delta R = 0.4, 0.7$. The parton-jet matching has been performed following the MLM prescription [29].⁶ We have not included detector effects in our analysis, except for a simple gaussian smearing on

⁵The factorization and renormalization scales have been chosen as follows: $\mu = M_{T,B}$ for the signal; $\mu = 2m_t + m_W$ for $t\bar{t}W + jets$; $\mu = 2m_t + m_h$ for $t\bar{t}WW + jets$; $\mu = m_W + m_h$ for $WWW + jets$; $\mu = 2m_W$ for $W^\pm W^\pm + jets$.

⁶The full chain of steps in the simulation process (linking MadGraph/MadEvent to Pythia, calling of Pythia, jet matching and jet reconstruction) has been performed using the package of dedicated programs in the MadGraph/MadEvent distribution [30].

	σ [fb]	$\sigma \times BR(l^\pm l^\pm)$ [fb]
$T_{5/3}\overline{T}_{5/3}/B\overline{B} + jets$ ($M = 500$ GeV)	2.5×10^3	104
$T_{5/3}\overline{T}_{5/3}/B\overline{B} + jets$ ($M = 1$ TeV)	37	1.6
$t\bar{t}W^+W^- + jets$ ($\supset t\bar{t}h + jets$)	121	5.1
$t\bar{t}W^\pm + jets$	595	18.4
$W^+W^-W^\pm + jets$ ($\supset hW^\pm + jets$)	603	18.7
$W^\pm W^\pm + jets$	340	15.5

Table 1: Signal and background cross sections at leading order (left column). The right column reports the cross section times the branching ratio to two same-sign leptons final states (e or μ).

the jets (we have smeared both the jet energy and momentum absolute value by $\Delta E/E = 100\%/\sqrt{E/\text{GeV}}$, and the jet momentum direction using an angle resolution $\Delta\phi = 0.05$ radians and $\Delta\eta = 0.04$).

The production cross sections for the signal and for the various backgrounds are reported in Table 1.⁷ No K-factors have been included, since those for the backgrounds are not all available (the K-factor for the signal is $\simeq 1.8$ (1.6) for $M = 0.5$ (1) TeV [31]). Given its complexity, we were not able to fully simulate the $Wl^+l^- + jets$ background, and for that reason we have not included it in our analysis. We have however estimated it as follows. First, one of the leptons coming from the l^+l^- pair in $Wl^+l^- + jets$ has to be missed in order for this process to lead to a same-sign dilepton final state. A lepton is considered missed if it goes outside the electromagnetic calorimeter or the muon chambers ($\eta > 2.5$), or if it is too soft to be detected (see for example [32]). In particular, if the lepton is missed because it is soft, it can be arbitrarily close to its companion in the l^+l^- pair, leading to a logarithmically enhanced collinear contribution if the pair originates from a virtual photon. A naive estimate based on the similar but simpler process $gg, q\bar{q} \rightarrow q\bar{q}l^+l^-$ indicates that, despite this log enhancement in the soft region, the contribution from the photon is much smaller than that from the Z , after the cuts on the missed lepton are applied.⁸ From the $WZ + jets$ cross section we thus expect the $Wl^+l^- + jets$ background to be smaller than $\sim 10 - 20\%$ of the sum of the other backgrounds. This includes a $\sim 10\%$ efficiency due to the lepton veto. While this estimate shows that $Wl^+l^- + jets$ is not entirely negligible, the error due to its exclusion is within the uncertainty of our leading-order analysis. Moreover,

⁷ Due to CPU limitations, in the case of the $WWW + jets$ and $W^\pm W^\pm + jets$ backgrounds we were not able to generate with MadGraph/MadEvent all the partonic multiplicities required for a 5 jets analysis. In particular, we generated (and matched) the following partonic processes: WWW , $WWWj$, $WWWjj$, and $W^\pm W^\pm jj$, $W^\pm W^\pm 3j$, $W^\pm W^\pm 4j$, with $j = \text{quark or gluon}$ (notice that the processes $pp \rightarrow W^\pm W^\pm$ and $pp \rightarrow W^\pm W^\pm j$ do not exist due to the conservation of the electric charge). This means that of the 5 hard jets required in the analysis, one will necessarily originate from Pythia. This leads to a slight underestimation of these backgrounds, which is however negligible in our analysis, since $WWW + jets$ and $W^\pm W^\pm + jets$ are largely subdominant after imposing the main cuts of the next section. In the case of the leading backgrounds $t\bar{t}W + jets$ and $t\bar{t}WW + jets$ all the required partonic multiplicities were instead generated.

⁸We thank Mauro Moretti for pointing this out and for correcting an error in our previous estimate.

the $Wl^+l^- + jets$ cross section is expected to be strongly suppressed after requiring the reconstruction of one W and one top as done in section 6.

Another potential source of background are $t\bar{t} + jets$ events where the charge of one of the two leptons from the top decays is misidentified. Given the large $t\bar{t} + jets$ cross section, even a charge misidentification probability $\varepsilon_{mis} \sim \text{a few} \times 10^{-3}$ would result into a same-sign dilepton background of the same order of $t\bar{t}W + jets$.⁹ The value of ε_{mis} strongly depends on the p_T and on the pseudo-rapidity of the lepton, and it is typically smaller for muons than for electrons. We find that the hardest lepton in the $t\bar{t} + jets$ events has a p_T distribution peaked at values smaller than 100 GeV (the second hardest lepton has instead a significantly softer p_T distribution). For such low- p_T leptons we have not found accurate estimates of ε_{mis} in the literature (studies on charge misidentification usually focus on leptons with very large p_T , from several hundred GeV to a few TeV, for which ε_{mis} is larger). From the latest ATLAS and CMS TDRs, probabilities as low as $\sim 10^{-4}$ seem to be realistic in the case of muons, while slightly larger values are expected for electrons [33, 34]. If $\varepsilon_{mis} = 10^{-4}$, the $t\bar{t} + jets$ background would be smaller by one order of magnitude than the dominant $t\bar{t}W + jets$ background in Table 1, hence safely negligible. In absence of a realistic estimate of ε_{mis} as a function of the lepton's p_T and pseudo-rapidity, we decided not to include the $t\bar{t} + jets$ background events in our analysis. It is however clear that a specific and accurate estimate of this background is required to validate our results.

Finally, it is worth commenting on the possible background due to possible additional leptons coming from b decays (that were not taken into account in our analysis). These leptons have a very soft p_T spectrum, so that the cuts imposed in section 5 on the lepton transverse momentum (we require $p_T > 25$ GeV for the softest lepton), together with the isolation cut $\Delta R_{lj} > 0.4$ between any lepton and jet, are expected to reduce such background to safely negligible levels.

4 Defining our Strategy

In this section we illustrate our strategy for the analysis of same-sign dilepton events. A first important information on the kinematics of signal and background events comes from the number of reconstructed jets, showed in Fig. 4 for two different choices of the cone size: $\Delta R = 0.4, 0.7$. For $\Delta R = 0.4$, the largest fraction of signal events have 5 or 6 jets, both in the case of $M = 500$ GeV and of $M = 1$ TeV (by signal here we mean either $T_{5/3}\bar{T}_{5/3}$ or $B\bar{B}$ events), while the total background distribution is peaked at smaller values (this is mainly due to the low jet multiplicity in the $WWW + jets$ and $W^\pm W^\pm + jets$ backgrounds). In the case of the signal, the hard scattering process produces 6 quarks, after the decay of the top and of the W . It turns out that for $M = 500$ GeV the 5-jet bin is mostly populated by events where the 6th jet is lost because it is too soft (i.e. it does not meet the minimum transverse energy requirement, $E_T \geq 30$ GeV), whereas for $M = 1$ TeV the 5-jet bin mainly contains events in which two jets coming from a boosted W decay have merged into a single jet. This is clearly illustrated in Fig. 5, which shows the invariant mass spectrum of the hardest and next-to-hardest jet. For $M = 1$ TeV the invariant mass of the hardest jet has

⁹Requiring the reconstruction of one W and one top as in section 6 is however expected to reduce significantly more the $t\bar{t} + jets$ events background than $t\bar{t}W + jets$ or $t\bar{t}WW + jets$.

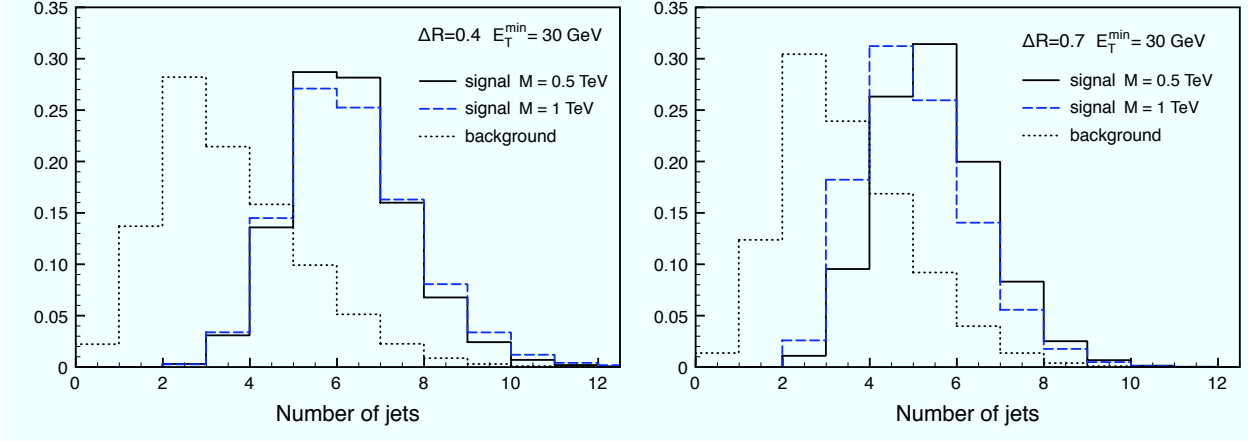


Figure 4: Fractions of signal and background events with a given number of jets for $E_T^{\min} = 30$ GeV and two different jet cone sizes: $\Delta R = 0.4$ (left plot), and $\Delta R = 0.7$ (right plot).

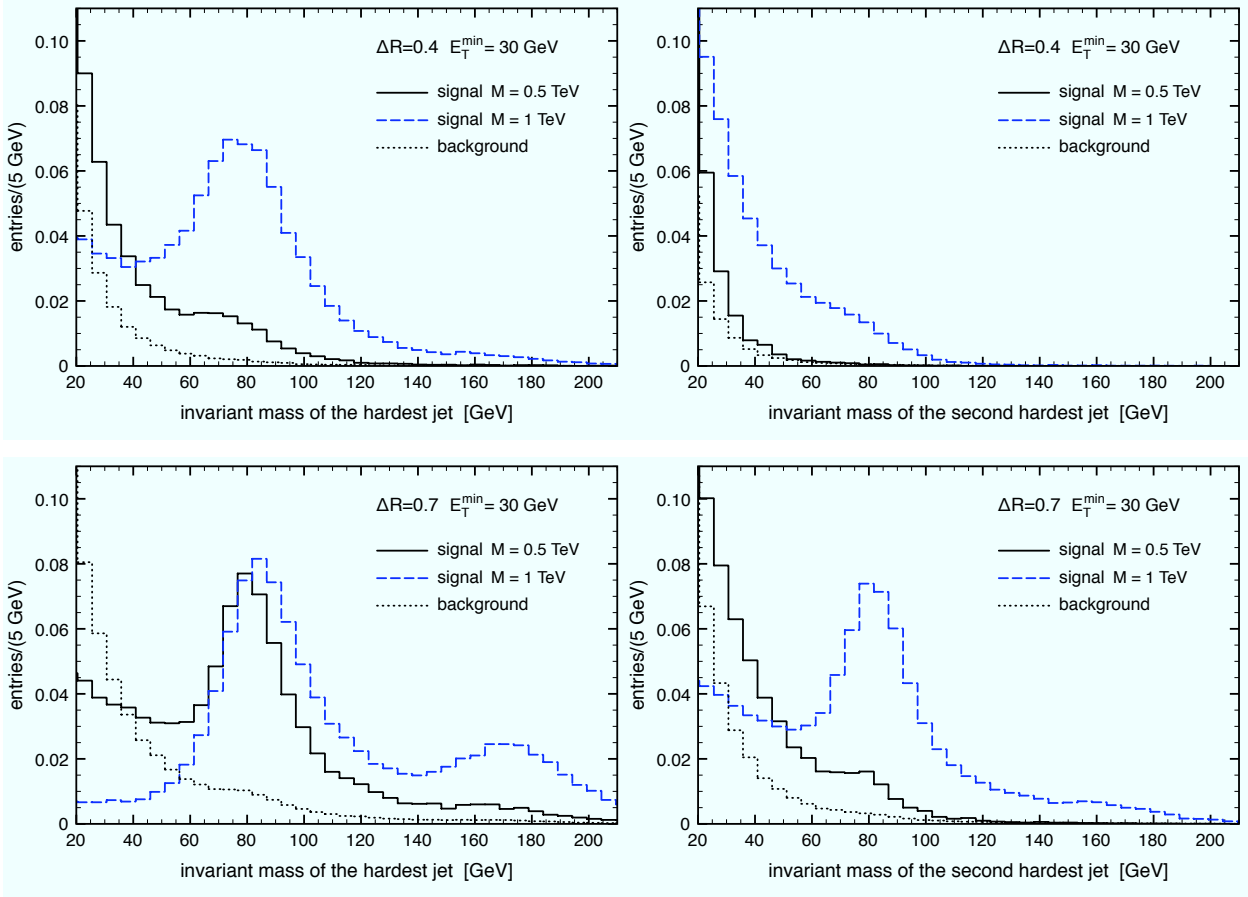


Figure 5: Invariant mass of the first (left) and second (right) hardest jet for $\Delta R = 0.4$ (top) and $\Delta R = 0.7$ (bottom). All distributions are normalized to unit area.

a peak in correspondence to m_W , while such a peak is absent in the case of $M = 500$ GeV, as well as in the distributions of the second hardest jet. We thus conclude that for a cone size $\Delta R = 0.4$, signal events with $M = 1$ TeV have one “double” jet, while background and $M = 500$ GeV signal events have none.

If one enlarges the cone size to $\Delta R = 0.7$, the most populated bins in the distributions of Fig. 4 (right plot) are those with 4 and 5 reconstructed jets. This suggests that in this case, both for $M = 1$ TeV and $M = 500$ GeV, another pair of closeby jets, originating from the decay of the second hadronic W decay, is merged into a single, double jet. This is again clearly illustrated in Fig. 5 (bottom plots), where one can see that signal events with $M = 500$ GeV have one double jet with $M_j \simeq m_W$, while those with $M = 1$ TeV have two. There are even cases, for $M = 1$ TeV, where all three jets from the hadronic decay of the top merge into a single jet with $M_j \simeq m_t$, see the left bottom plot of Fig. 5. We find, however, that the fraction of these “triple” top jets is relatively small.

Identifying and selecting events with one triple and one double jet was the strategy adopted in Ref. [21] to discover and reconstruct heavy bottoms with $M = 1$ TeV (see also Refs. [35–39, 18] where a similar jet-mass technique was applied to different processes). According to the authors of Ref. [21], the presence of these massive jets can discriminate the events of the signal from those of the background. In particular, an excess of more than 5σ compared to the SM prediction can be obtained with $L = 100 \text{ fb}^{-1}$ by counting the number of jets with $M_j \sim m_W$. This evidence alone, however, is not per se an indication that a heavy B has been produced (the boosted W could arise from a different process), and it has to be accompanied by a full reconstruction of the B invariant mass.¹⁰

The effective validity of such a single-jet mass technique seems to depend significantly on the adopted jet algorithm and the value of its parameters. The k_T algorithm [40] was chosen in Ref. [21]. As the plots of Fig. 5 show, at least one double or triple jet can be resolved into individual jets by using a cone algorithm with $\Delta R = 0.4$. Resolving as many jets as possible seems to be a better option than choosing a larger cone size and imposing only jet-mass constraints: First, because in the former case the QCD background will have a larger jet multiplicity (one or two jets more), hence a smaller cross section to begin with. Second, because the requirement of having two closeby jets (in our specific case with $\Delta R_{jj} < 0.7$) with an invariant mass $M_j \simeq m_w$ (or $M_j \simeq m_t$) should be as effective as – if not more effective than – the cut on the invariant mass of the corresponding double (or triple) jet. Clearly, measuring the single-jet mass, as well as analyzing the jet substructure [35, 37],¹¹ remain promising strategies for the cases in which the double jet cannot be resolved.

For the reasons explained above, we decided to perform our analysis setting the cone size to $\Delta R = 0.4$, and to require at least 5 reconstructed jets in the final state, both for $M = 500$ GeV and $M = 1$ TeV. Even in the case of $M = 1$ TeV, where the signal has typically one double jet, we preferred not to impose any cut on the single-jet invariant mass, trying to develop a strategy as independent as possible of the details of the detector and of the jet algorithm. In this sense our results are somehow conservative, as one can hope to eventually improve on them by making use of jet mass cuts.

¹⁰ The invariant mass distribution of the Wt system is presented in Ref. [21] only for final states with one lepton, without however quoting the statistical significance of the resonant peak.

¹¹ See also [41, 42] for the related issue of the identification of highly boosted tops.

	signal ($M = 500$ GeV)	signal ($M = 1$ TeV)	$t\bar{t}W$	$t\bar{t}WW$	WWW	$W^\pm W^\pm$
Efficiencies (ε_{main})	0.42	0.43	0.074	0.12	0.008	0.01
$\sigma [\text{fb}] \times BR \times \varepsilon_{main}$	44.2	0.67	1.4	0.62	0.15	0.16

Table 2: Efficiencies of the main cuts of eq.(8). Here signal means either $T_{5/3}\bar{T}_{5/3}$ or $B\bar{B}$ events.

5 Discovery Analysis

In this section and in the next one we present our main analysis of same-sign dilepton events. We focus first on the discovery of the top partners, proposing a simple strategy that does not rely on any sophisticated reconstruction, nor does it require b -tagging. We will adopt $L = 10 \text{ fb}^{-1}$ ($L = 100 \text{ fb}^{-1}$) as a reference integrated luminosity for the various plots in the case $M = 500 \text{ GeV}$ ($M = 1 \text{ TeV}$), and we will consider two different scenarios (or “models”): in the first, both B and the exotic $T_{5/3}$ are present with the same mass M ; in the second, only B exists.¹²

Our main cuts to isolate the signal are the followings:

$$\begin{array}{l} \underline{2 \text{ same-sign}} \\ \underline{\text{leptons}} \\ \underline{(e \text{ or } \mu)} \end{array} : \begin{cases} p_T(1\text{st}) \geq 50 \text{ GeV} \\ p_T(2\text{nd}) \geq 25 \text{ GeV} \\ |\eta_l| \leq 2.4, \quad \Delta R_{lj} \geq 0.4 \end{cases} \quad \underline{\text{jets}} : \begin{cases} p_T(1\text{st}) \geq 100 \text{ GeV} \\ p_T(2\text{nd}) \geq 80 \text{ GeV} \\ n_{jet} \geq 5, \quad |\eta_j| \leq 5 \end{cases} \quad \cancel{E}_T \geq 20 \text{ GeV}, \quad (8)$$

where 1st and 2nd refer respectively to the first and second hardest jet or lepton (electron or muon). The relative efficiencies are reported in Table 2.

For 500 GeV masses, the signal is so much larger than the background after the cuts of eq.(8) that a plot of the total invariant mass of the jets and the leptons (that is: the total invariant mass of the event, excluding the missing energy) gives a clear and striking evidence for a resonant production at $M_{inv}(\text{tot}) = 2M$, see Fig. 6. Moreover, by plotting the invariant mass of the hardest 5 jets one gets the additional indication of the presence of a resonance at $M_{inv}(5j) \sim M$ in the scenario with $T_{5/3}$, see right upper plot of Fig. 6. Although this latter resonant peak is also quite evident, it is centered at values slightly larger than the true $T_{5/3}$ mass, suggesting that the hardest 5 jets not always coincide with those originating from the hadronic decay of the new heavy fermion. A better resolution of the $T_{5/3}$ mass can be obtained by demanding two b tags, and plotting the invariant mass of the hardest 4 jets plus the b -jet that has the largest ΔR with the softest lepton. This last requirement is useful to reduce the combinatorial background eliminating the b from the semileptonic decay of the top, as the latter is typically very boosted and its decay products emerge in a small angular cone. The dotted and dashed curves in the right upper plot of Fig. 6 show the invariant mass distributions obtained in this way. No b -tagging efficiency factor has been included,¹³ in order not to commit to any specific value. Since typical b -tagging efficiencies

¹²The case where $T_{5/3}$ is much lighter than B is disfavored by electroweak precision data [24].

¹³The b -tagging algorithm that we have used, from the MadGraph/MadEvent distribution [30], has an intrinsic tagging efficiency that we have however rescaled out.

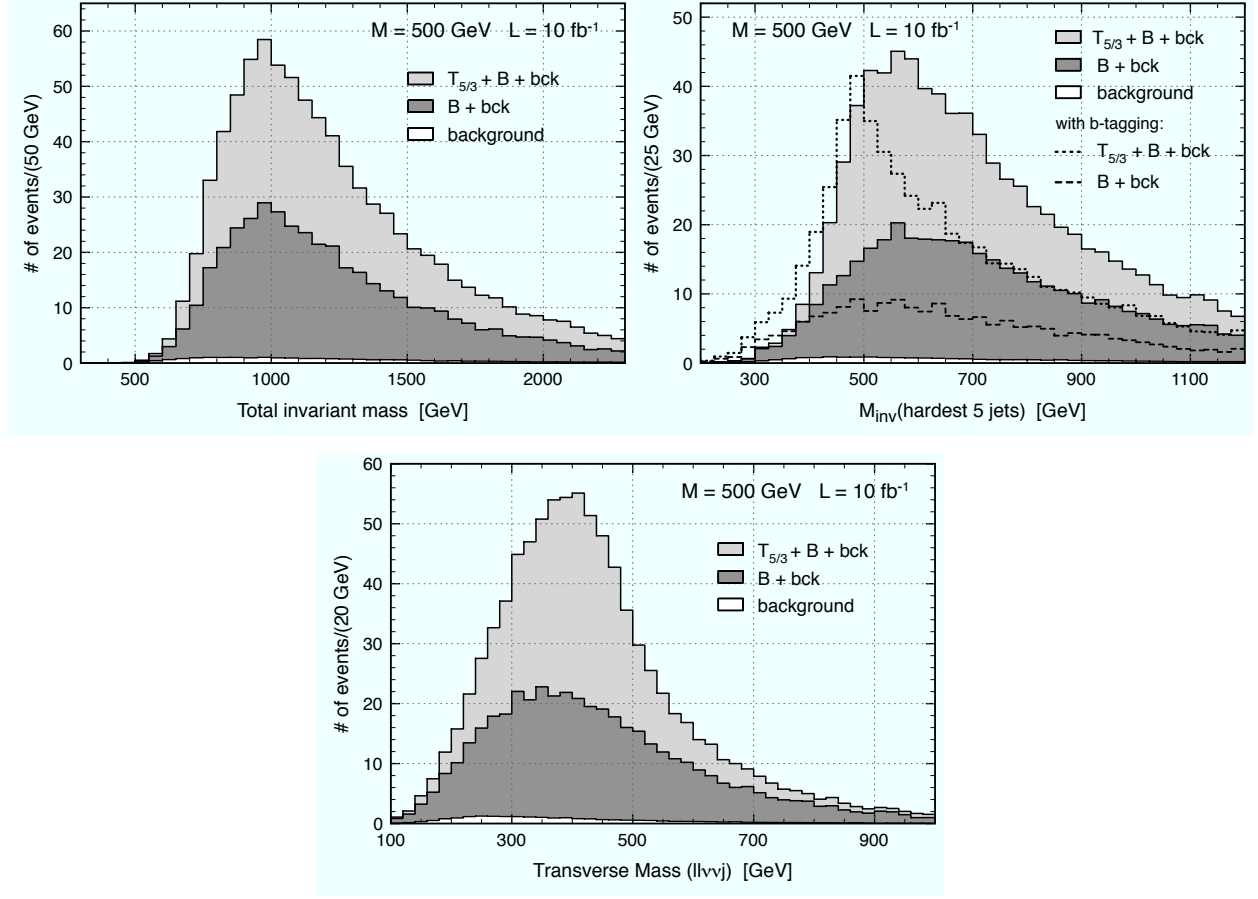


Figure 6: Distributions after the main cuts of eq.(8) for $M = 500 \text{ GeV}$: *a*) Total invariant mass (upper left plot); *b*) Invariant mass of the hardest 5 jets (upper right plot); *c*) Transverse invariant mass of the system ($ll\nu\nu j$), see text (lower plot). The dotted and dashed curves in *b*) correspond to the invariant mass of the hardest 4 jets plus the b -jet that has the largest ΔR with the softest lepton. They assume two b tags, though no b -tagging efficiency has been included, see text.

at the LHC are of the order $\varepsilon_b \sim 0.5$, the final distribution will be rescaled by a factor $\varepsilon_b^2 \sim 0.25$, suggesting that b -tagging is probably not worth in the initial discovery phase, but it will be quite effective to obtain a better mass resolution after having accumulated sufficient statistics.

Finally, some further crucial information on the kinematics of the events comes from the two same-sign leptons. In the case of the $T_{5/3}\bar{T}_{5/3}$ events, one would like to reconstruct the leptonic decay of the second heavy fermion, although this is complicated by the presence of two neutrinos. Here we consider only a very simple reconstruction procedure, leaving more sophisticated approaches to future analyses. Figure 6, bottom plot, shows the transverse invariant mass of the system [two leptons + two neutrinos + jet closest to the softest lepton] – where “closest” here means “with the smallest ΔR ” – defined as

$$M_T^2(ll\nu\nu j) = (E_T(llj) + E_T(\nu\nu))^2 - |\vec{p}_T(llj) + \vec{p}_T(\nu\nu)|^2, \quad (9)$$

$$E_T(llj) \equiv \sqrt{|\vec{p}_T(llj)|^2 + M_{inv}^2(llj)}, \quad E_T(\nu\nu) \equiv |\vec{p}_T(\nu\nu)|.$$

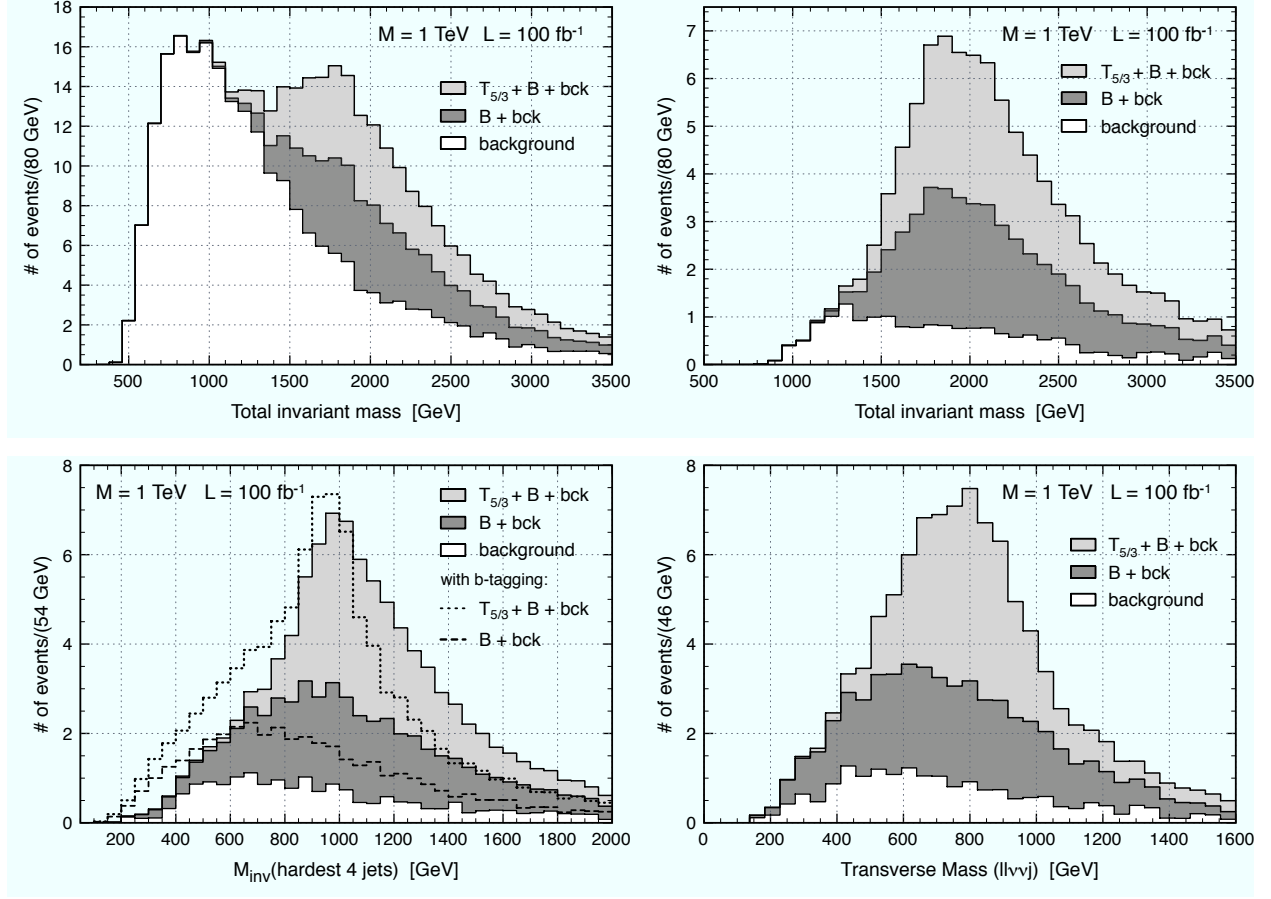


Figure 7: Distributions for $M = 1$ TeV: a) Total invariant mass after the main cuts of eq.(8) (upper left plot); b) Total invariant mass after the extra cuts of eq.(10) (upper right plot); c) Invariant mass of the hardest 4 jets, after the extra cuts of eq.(10) (lower left plot); d) Transverse invariant mass of the system ($ll\nu\nu j$), after the extra cuts of eq.(10), see text (lower plot). The dotted and dashed curves in c) correspond to the invariant mass of the hardest 3 jets plus the b -jet that has the largest ΔR with the softest lepton. They assume two b tags, though no b -tagging efficiency has been included, see text.

In the scenario with $T_{5/3}$ partners, the transverse mass distribution has an approximate edge at $M_T(ll\nu\nu j) \sim M$ due to the resonant leptonic decay,¹⁴ while it is smoother in the other scenario with only the B (where no resonance is expected in the system of the two leptons).

For 1 TeV masses the SM background is still larger than the signal after the cuts of eq.(8), but the resonant peak at $M_{inv}(\text{tot}) = 2M$ is already distinguishable in the total invariant mass distribution, see the upper left plot of Fig. 7. To further reduce the background and isolate the resonance we have performed the following extra “discovery” cuts:

$$p_T(\text{1st jet}) \geq 200 \text{ GeV}, \quad \sum_{i=1,2} |\vec{p}_T(l_i)| \geq 300 \text{ GeV}. \quad (10)$$

¹⁴ The edge is only approximate because of the omission of the unknown invariant mass of the system of the two neutrinos in the definition (9).

	signal ($M = 1 \text{ TeV}$)	$t\bar{t}W$	$t\bar{t}WW$	WWW	WW
Efficiencies (ε_{disc})	0.65	0.091	0.032	0.16	0.18
$\sigma [\text{fb}] \times BR \times \varepsilon_{main} \times \varepsilon_{disc}$	0.43	0.12	0.02	0.02	0.03

Table 3: Efficiencies of the extra “discovery” cuts of eq.(10) for the case $M = 1 \text{ TeV}$. Here signal means either $T_{5/3}\bar{T}_{5/3}$ or $B\bar{B}$ events.

		\mathcal{S}	\mathcal{B}	L_{disc}
$M = 500 \text{ GeV}$	$T_{5/3} + B$	864	23	56 pb^{-1}
	$B \text{ only}$	424	23	147 pb^{-1}
$M = 1 \text{ TeV}$	$T_{5/3} + B$	83	19	15 fb^{-1}
	$B \text{ only}$	40	19	48 fb^{-1}

Table 4: Number of signal (\mathcal{S}) and background (\mathcal{B}) events that pass the main cuts of eq.(8) (eq.(8) and eq.(10)) with $L = 10 \text{ fb}^{-1}$ ($L = 100 \text{ fb}^{-1}$) for $M = 500 \text{ GeV}$ ($M = 1 \text{ TeV}$). The last column reports the corresponding integrated luminosity needed for the discovery (L_{disc}), as computed by means of a goodness-of-fit test with Poisson distribution and p-value = 2.85×10^{-7} (see text).

The corresponding efficiencies are reported in Table 3. After these cuts, similarly to the 500 GeV case, finding the correlated resonant peaks in the total invariant mass and in the invariant mass of the hardest 4 jets would give strong indication that a pair of $T_{5/3}$ has been produced with mass $M = 1 \text{ TeV}$. This could be further confirmed by the transverse mass distribution of the $(ll\nu\nu j)$ system. The presence of a resonant peak only in the total invariant mass would instead give evidence for a $B\bar{B}$ pair production. All these distributions are reported in Fig. 7. Notice that, differently from the 500 GeV case, here we have plotted the invariant mass of the hardest 4 (not 5) jets, since, as showed in section 4, for $M = 1 \text{ TeV}$ the signal typically contains one double jet from a boosted W decay. Accordingly, the dotted and dashed curves in plot *c*) of Fig. 7, obtained by requiring two b -tags, correspond to the invariant mass of the hardest 3 jets plus the b -jet that has the largest ΔR with the softest lepton.

By counting the number of signal and background events that pass the main cuts of eq.(8) (plus those of eq.(10) in the $M = 1 \text{ TeV}$ case), one can estimate the statistical significance of the signal over the background, as well as the minimum integrated luminosity required for a discovery. We define the latter to be the integrated luminosity for which a goodness-of-fit test of the SM-only hypothesis with Poisson distribution gives a p-value = 2.85×10^{-7} [43].¹⁵ Our results are reported in Table 4. In the most favorable case where both $T_{5/3}$ and B partners exist and have mass $M = 500 \text{ GeV}$, a discovery will need only $\sim 56 \text{ pb}^{-1}$. In the 1 TeV case, the theoretical uncertainty on the SM background can reduce the significance of the observed excess. Nevertheless, our estimates should still be conservative as we did not include any

¹⁵This p-value corresponds to a 5σ significance in the limit of a gaussian distribution.

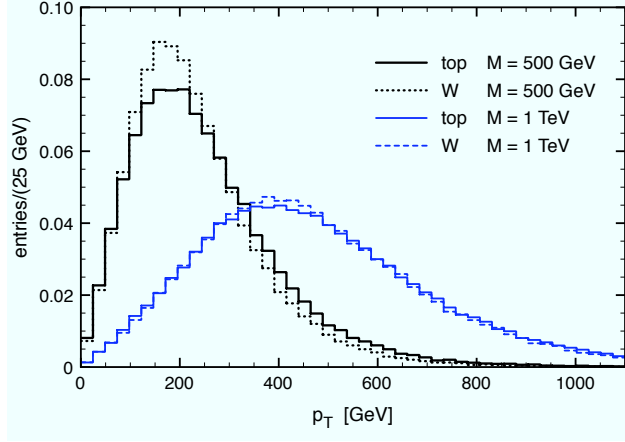


Figure 8: Distributions of the p_T of the W and t in signal events, normalized to unit area.

	signal ($M = 500$ GeV)	$t\bar{t}W$	$t\bar{t}WW$	WWW	WW
ε_{2W}	0.62	0.36	0.49	0.29	0.15
ε_{top}	0.65	0.56	0.64	0.35	0.35

Table 5: Individual efficiencies for the reconstruction of two W 's (ε_{2W}) and one top (ε_{top}) using the algorithm and the cuts described in the text for the case $M = 500$ GeV. The total efficiency for the top reconstruction is $\varepsilon_{2W} \times \varepsilon_{top}$.

K-factor in our analysis, although it is known that next-to-leading order corrections enhance the signal cross section by $\sim 80\%$ ($\sim 60\%$) for $M = 500$ GeV ($M = 1$ TeV) [31]. Even a common K-factor κ for both the signal and the background would imply a statistical significance larger by a factor $\sim \sqrt{\kappa}$, as well as a discovery luminosity smaller by the same factor. After an excess of events has been established, the compatibility with B or $T_{5/3}$ pair production can be demonstrated using the shapes of the signal distributions of Fig. 6 and 7 for a given value of the mass.

6 Mass Reconstruction

More direct evidence for the production of a pair of $T_{5/3}$ or B comes from reconstructing the hadronically decayed top quark and W boson, as well as from the distribution of the invariant mass of their system.

In the $M = 500$ GeV case, we first select the events where two W 's can be simultaneously reconstructed, each W candidate being formed by a pair of jets with invariant mass in the window $|M(jj) - m_W| \leq 20$ GeV. To avoid wrong pairings and reduce the fake ones from

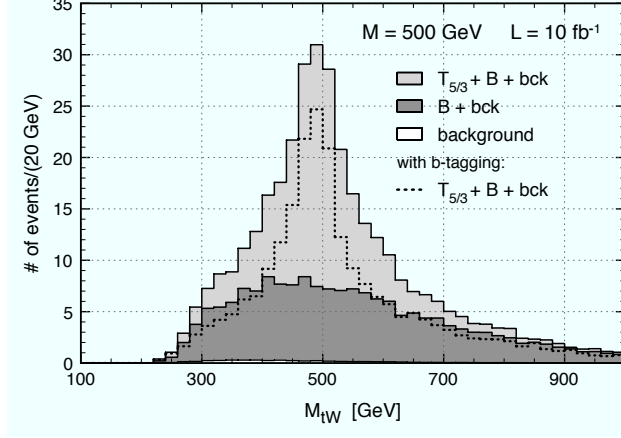


Figure 9: Invariant mass of the Wt system for $M = 500$ GeV with $L = 10 \text{ fb}^{-1}$. The dotted curve refers to the case in which b -tagging is performed in the reconstruction, see text. It assumes two b tags, though no b -tagging efficiency has been included.

the background, we impose the following cuts:

$$\Delta R_{jj} \leq 1.5, \quad |\vec{p}_T(W)| \geq 100 \text{ GeV} \quad \text{on the first } W \text{ candidate}; \quad (11)$$

$$\Delta R_{jj} \leq 2.0, \quad |\vec{p}_T(W)| \geq 30 \text{ GeV} \quad \text{on the second } W \text{ candidate}. \quad (12)$$

The p_T cuts, in particular, have been optimized using the distributions of Fig. 8. If more than one pair of W candidates exists which satisfies the above cuts, we select that with the smallest $\chi^2 = \Delta R_{jj}^2(\text{1st pair}) + \Delta R_{jj}^2(\text{2nd pair})$. We then reconstruct the top by forming Wj pairs, made of one W and one of the remaining jets, with invariant mass in the window $|M(Wj) - m_t| \leq 25 \text{ GeV}$. If more than one top candidate exists, we select that with invariant mass closest to m_t . We discard events where no top can be reconstructed. The efficiencies of this reconstruction algorithm are reported in Table 5.

The distribution of the Wt invariant mass is plotted in Fig. 9. As expected, in the scenario with $T_{5/3}$ partners there is a resonant peak centered at $M_{T_{5/3}} = 500 \text{ GeV}$, while the distribution has a non-resonant, continuous shape if only $Q_e = -1/3$ heavy fermions exist. The dotted curve refers to the case in which b -tagging is performed in the reconstruction algorithm. In more detail, we have selected events with two b tags and we have reconstructed the top from Wb pairs, excluding at the same time the b jets when selecting the W jet pair candidates. As before, no b -tagging efficiency has been included.

In the 1 TeV case the algorithm for the reconstruction of W and t has to be modified, to take into account that signal events often contain one double jet, as shown in section 4. As the various reconstruction requirements will themselves reduce the background, we can start our analysis imposing a set of extra cuts, in addition to those of eq.(8), that is less aggressive than those demanded in eq.(10) for the discovery. We require:

$$M_{inv}(\text{tot}) \geq 1500 \text{ GeV}, \quad \begin{cases} p_T(\text{1st jet}) \geq 200 \text{ GeV} \\ p_T(\text{2nd jet}) \geq 100 \text{ GeV} \end{cases}, \quad p_T(\text{1st lepton}) \geq 100 \text{ GeV}. \quad (13)$$

	signal ($M = 1$ TeV)	$t\bar{t}W$	$t\bar{t}WW$	WWW	WW
Efficiencies (ε_{rec})	0.83	0.18	0.07	0.22	0.38
$\sigma [\text{fb}] \times BR \times \varepsilon_{main} \times \varepsilon_{rec}$	0.55	0.24	0.04	0.03	0.06

Table 6: Efficiencies of the extra “reconstruction” cuts of eq.(13) for the case $M = 1$ TeV. Here signal means either $T_{5/3}\bar{T}_{5/3}$ or $B\bar{B}$ events.

	signal ($M = 1$ TeV)	$t\bar{t}W$	$t\bar{t}WW$	WWW	WW
ε_{2W}	0.31	0.15	0.23	0.16	0.071
ε_{1W}	0.57	0.62	0.59	0.58	0.49
$\varepsilon_{top}^{[2W]}(t = Wj)$	0.62	0.56	0.62	0.11	0.13
$\varepsilon_{top}^{[1W]}(t = Wj)$	0.44	0.56	0.53	0.22	0.20
$\varepsilon_{top}(t = jj)$	0.18	0.04	0.06	0.06	0.07

Table 7: Efficiencies of the algorithms and the cuts described in the text for the case $M = 1$ TeV: reconstruction of two (ε_{2W}) or one (ε_{1W}) W ’s; reconstruction of the top as Wj using events with two ($\varepsilon_{top}^{[2W]}(t = Wj)$) or one ($\varepsilon_{top}^{[1W]}(t = Wj)$) W ’s; reconstruction of the top from a pair of jets ($\varepsilon_{top}(t = jj)$).

The corresponding efficiencies are reported in Table 6. We design our strategy so as to be successful in three different situations: *i*) no double jet is present in the event; *ii*) there is one double jet corresponding to the W boson emitted in the primary decay of the heavy fermion; *iii*) there is one double jet originating from the decay of the top quark. In the first case the reconstruction can proceed as for $M = 500$ GeV, using events with two reconstructed W ’s; in the last two cases instead, the presence of one double jet implies that only one W should be required. We thus divide the events into two samples as follows: those in which two W ’s can be reconstructed, each made of a pair of jets with $|M(jj) - m_W| \leq 20$ GeV; and those where only one W can be reconstructed. The two W candidates of each event in the first sample are required to satisfy the following cuts:

$$\Delta R_{jj} \leq 0.7, \quad |\vec{p}_T(W)| \geq 250 \text{ GeV} \quad \text{on the first } W \text{ candidate}; \quad (14)$$

$$\Delta R_{jj} \leq 1.5, \quad |\vec{p}_T(W)| \geq 80 \text{ GeV} \quad \text{on the second } W \text{ candidate}. \quad (15)$$

Events of the second sample are instead selected imposing the cuts of eq.(15) on their W candidate. The efficiencies for the reconstruction of two and one W (equal to the percentage of the total events classified respectively in the first and second sample) are reported in Table 7.

We thus reconstruct one top from Wj pairs with $|M(Wj) - m_t| \leq 25$ GeV, as for $M =$

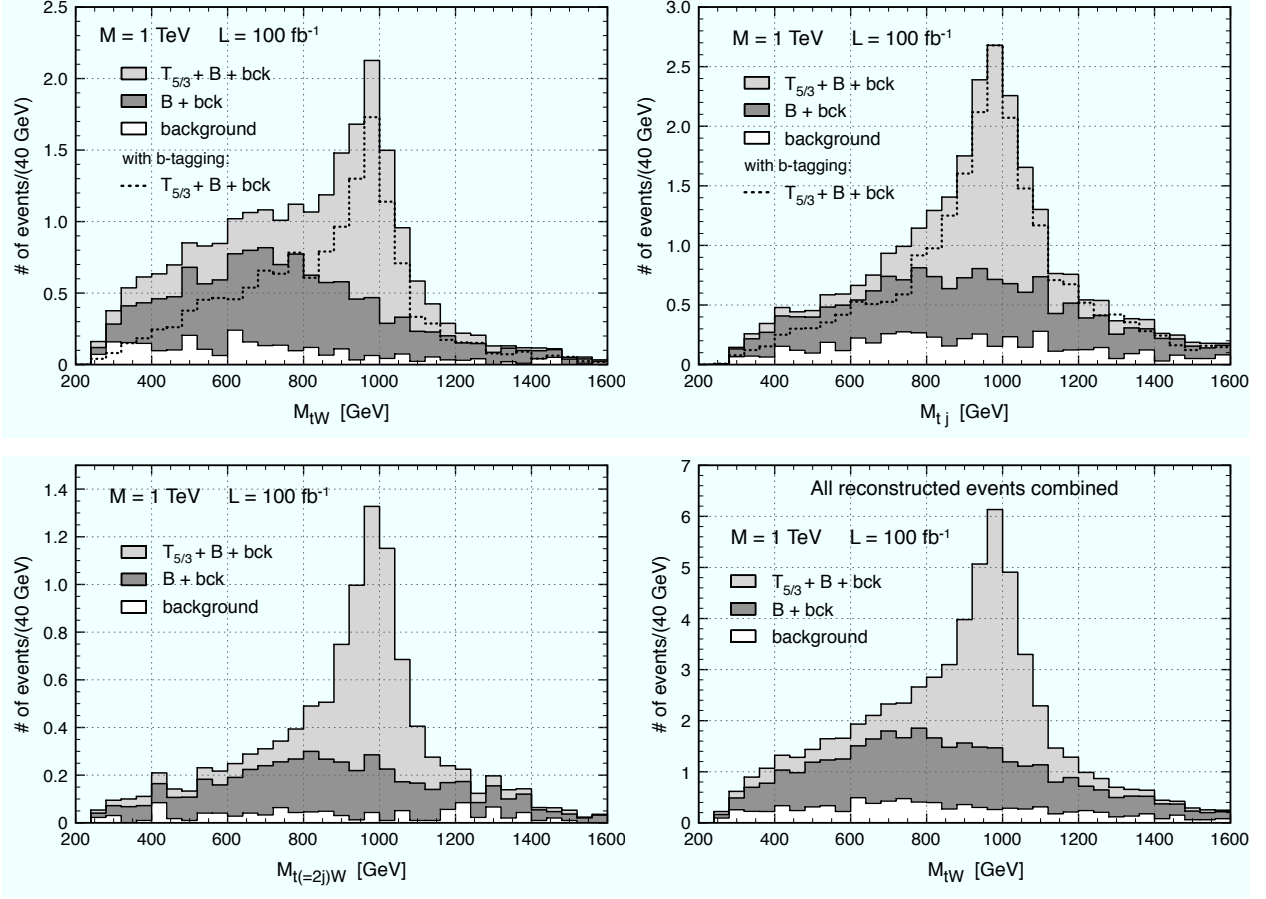


Figure 10: Invariant mass of the Wt system, for $M = 1 \text{ TeV}$ and $L = 100 \text{ fb}^{-1}$, obtained following the three reconstruction procedures described in the text (first three plots). The dotted curves in the first and second plot show the effect of performing the b -tagging in the top reconstruction. They assume two b tags, though no b -tagging efficiency has been included. The lower right plot shows the total Wt distribution obtained by combining the events of the first three plots.

500 GeV, using events of the first sample (those with two W 's). Events where no top can be reconstructed are removed. The corresponding efficiency, labeled as $\varepsilon_{top}^{[2W]}(t = Wj)$, is reported in Table 7. The final invariant mass of the Wt pair is plotted in Fig. 10, upper left plot. The dotted curve refers to the case in which b -tagging has been performed in the reconstruction, according to the same procedure adopted in the $M = 500 \text{ GeV}$ case.

Events from the second sample (those with one W) are used to reconstruct the top in two possible ways: first, the reconstruction is attempted selecting Wj pairs with $|M(Wj) - m_t| \leq 25 \text{ GeV}$; in case of unsuccess, we then try to reconstruct the top forming pairs of jets with $|M(jj) - m_t| \leq 25 \text{ GeV}$, where one of the two is assumed to be a double jet. If more than one top candidate exists, we select that with invariant mass closest to m_t . If instead none is found the event is removed. The efficiencies of these two reconstruction procedures, respectively labeled as $\varepsilon_{top}^{[1W]}(t = Wj)$ and $\varepsilon_{top}(t = jj)$, are reported in Table 7. Events with one W in which the top is reconstructed as Wj are those where the double jet corresponds to the W boson emitted in the heavy fermion primary decay. It turns out that such double jet is

usually the hardest among the remaining jets (those not involved in the top reconstruction). We thus plot the invariant mass of tj , where j is the hardest other jet with $p_T \geq 80$ GeV, see the upper right plot of Fig. 10. As before, the dotted curve shows the effect of performing the b -tagging in the top reconstruction. For events with one W and the top reconstructed from a pair of jets we plot instead the tW invariant mass, see the lower left plot of Fig. 10.

As illustrated in the first three plots of Fig. 10, all three different methods that we have described for reconstructing the hadronically decayed $T_{5/3}$ are quite successful: the resonant peak at $M_{T_{5/3}} = 1$ TeV is always clearly distinguishable over the non-resonant distribution due to the B . The presence of the peak would thus give the ultimate evidence in favor of the $T_{5/3}$, whereas its absence would rather indicate that a pair of B 's has been produced. To enhance the statistical significance, the events from the three plots can be combined into a single distribution, shown in the lower right plot of Fig. 10.

7 Discussion and Outlook

The results of sections 5 and 6 show that the analysis of final states with two same-sign leptons at the LHC is an extremely promising method to discover the top partners B and $T_{5/3}$. By requiring two same-sign leptons one avoids the large $t\bar{t}$ background and selects a particularly clean channel where evidence for the existence of the heavy fermions could come in the early phase of the LHC. The estimate of section 5 suggests that a discovery could be claimed already with $\sim 50 \text{ pb}^{-1}$ or $\sim 150 \text{ pb}^{-1}$ for $M = 500$ GeV, respectively if both B and $T_{5/3}$ or only B exist. Even without b -tagging, and before reconstructing the hadronically decayed W and top, one can have a first crucial indication on the value of the mass of the heavy fermions from the distributions of the total invariant mass and the invariant mass of the hardest 5 or 4 jets. The presence of a resonant peak in both distributions, respectively at $M_{inv}(\text{tot}) \sim 2M$ and $M_{inv}(\text{hardest 5 or 4 jets}) \sim M$, would be specific evidence for the production of the $T_{5/3}$.

Although the use of b -tagging can increase the resolution of the resonant peaks, hence their statistical significance, the ultimate evidence for the discovery of $T_{5/3}$ would come from its reconstruction in the Wt invariant mass. As our explorative study indicates, the strategy to follow in that case will need to be optimized according to the value of the heavy fermion mass M . In general, it will be preferable to suitably choose and tune the jet algorithm to individually resolve as many jets as possible. In the case of a cone algorithm, this means choosing a not too large cone size. We found that $\Delta R = 0.4$ gives good results, as it permits to resolve all the jets from the decay of the top and the W for $M = 500$ GeV, while only one double jet is typically present in the signal events for $M = 1$ TeV. In this respect our analysis differs from that of Ref. [21], where the proposed strategy to reconstruct 1 TeV heavy bottoms was that of selecting and pairing jets with invariant mass close to m_t and m_W . In the case of the B , its full reconstruction will be only possible by analyzing events with one or two opposite-sign leptons. For that purpose, the first rough indication on the value of M extracted from the same-sign dilepton events will serve to guide the analysis and optimize the cuts needed to kill the large SM background. In this sense, the use of all final states with different lepton multiplicities will permit to discriminate different scenarios where only one or both top partners exist.

Ultimately, a crucial information to understand the origin and the role of the heavy fermions would come from the measurement of their decay width, which will in turn lead to a determination of their couplings $\lambda_{T_{5/3},B}$. As already stressed before, a large value of $\lambda_{T_{5/3},B}$ will be strong circumstantial evidence for the compositeness of the heavy fermions. Extracting the decay width from the invariant mass distribution will be challenging, as one will have to cope with the issue of jet energy resolution. Most likely, a measurement will be possible only with large statistics and will require more sophisticated W and t reconstruction techniques.

In this analysis, we only considered the model-independent pair production of the top partners, neglecting their single production. At the LHC the latter proceeds through Wt fusion, via the diagram of Fig. 2, and leads to final states with $t\bar{t}W + jets$. It will thus contribute to the same-sign dilepton channel, enhancing the significance of the new physics signal over the SM background. Its effect will be more important for heavier masses M (for which the pair-production cross section is more suppressed) and larger couplings $\lambda_{T_{5/3},B}$. However, due to the absence of a second, hadronically decaying top partner, events from single production will not give a resonant contribution to the Wt invariant mass distribution, or to the invariant mass of the hardest 4 or 5 jets. In this sense, the inclusion of single production should not dramatically affect the results of our simplified analysis, and it could even lead to a larger statistical significance in the first discovery phase. It is clear, however, that a dedicated analysis will be required to assess the actual importance of single production, and to determine its potentialities in extending the LHC discovery reach for larger values of the heavy masses M .

Given the strong theoretical motivations for a search of the heavy partners of the top, we think that our explorative study would also deserve to be followed by a dedicated experimental investigation. Our results suggest that the same-sign dilepton channel might be one of the golden modes to discover the top partners B and $T_{5/3}$, but only a complete analysis with a full simulation of the detector effects, an exact calculation of the $Wl^+l^- + jets$ and $t\bar{t} + jets$ backgrounds, and the use of fully realistic reconstruction techniques will eventually establish its ultimate potentialities.

Acknowledgments

We thank A. Polosa for collaboration in the early stages of this project and for many useful discussions. We are indebted to M. Mangano and F. Maltoni for illuminating discussions and suggestions, and with J. Alwall, M. Herquet and all the CP3 team for their constant and absolutely crucial assistance on Madgraph. It is also a pleasure to thank J. A. Aguilar-Saavedra, D. Berge, G. Brooijmans, P. Ciafaloni, D. Del Re, S. Frixione, Y. Gershtein, M. Moretti, M. Narain, F. Piccinini, M. Pierini, R. Rattazzi, M. Spiropulu, and J. Tseng for several interesting and stimulating discussions and comments.

References

- [1] LEP Electroweak Working Group, <http://lepewwg.web.cern.ch>

- [2] S. Weinberg, Phys. Rev. Lett. **59** (1987) 2607.
- [3] V. Agrawal, S. M. Barr, J. F. Donoghue and D. Seckel, Phys. Rev. D **57** (1998) 5480 [arXiv:hep-ph/9707380].
- [4] N. Arkani-Hamed and S. Dimopoulos, JHEP **0506**, 073 (2005) [arXiv:hep-th/0405159].
- [5] S. Weinberg, Phys. Rev. Lett. **29** (1972) 1698.
- [6] H. Georgi and A. Pais, Phys. Rev. D **12**, 508 (1975).
- [7] D. B. Kaplan and H. Georgi, Phys. Lett. B **136** (1984) 183.
- [8] J. Maldacena, Adv. Theor. Math. Phys. **2**, 231 (1998) [arXiv:hep-th/9711200]; S. Guber, I. Klebanov and A. Polyakov, Phys. Lett. B **428**, 105 (1998) [arXiv:hep-th/9802109]; E. Witten, Adv. Theor. Math. Phys. **2**, 253 (1998) [arXiv:hep-th/9802150]; for a review see O. Aharony, S. Gubser, J. Maldacena, H. Ooguri and Y. Oz, Phys. Rept. **323**, 183 (2000) [arXiv:hep-th/9905111].
- [9] N. Arkani-Hamed, M. Porrati and L. Randall, JHEP **0108**, 017 (2001) [arXiv:hep-th/0012148]; R. Rattazzi and A. Zaffaroni, JHEP **0104**, 021 (2001) [arXiv:hep-th/0012248].
- [10] R. Contino, Y. Nomura and A. Pomarol, Nucl. Phys. B **671** (2003) 148 [arXiv:hep-ph/0306259].
- [11] P. Sikivie, L. Susskind, M. B. Voloshin and V. I. Zakharov, Nucl. Phys. B **173** (1980) 189.
- [12] K. Agashe, R. Contino, L. Da Rold and A. Pomarol, Phys. Lett. B **641** (2006) 62 [arXiv:hep-ph/0605341].
- [13] R. Contino, L. Da Rold and A. Pomarol, Phys. Rev. D **75**, 055014 (2007) [arXiv:hep-ph/0612048].
- [14] M. S. Carena, E. Ponton, J. Santiago and C. E. M. Wagner, Nucl. Phys. B **759** (2006) 202 [arXiv:hep-ph/0607106]; A. D. Medina, N. R. Shah and C. E. M. Wagner, Phys. Rev. D **76** (2007) 095010 [arXiv:0706.1281 [hep-ph]].
- [15] G. Panico, E. Ponton, J. Santiago and M. Serone, arXiv:0801.1645 [hep-ph].
- [16] See also: G. Cacciapaglia, C. Csaki, G. Marandella and J. Terning, Phys. Rev. D **75** (2007) 015003 [arXiv:hep-ph/0607146]; G. Cacciapaglia, C. Csaki, G. Marandella and J. Terning, JHEP **0702** (2007) 036 [arXiv:hep-ph/0611358], for models that incorporate the P_{LR} protection but where the Higgs is either absent or not a pseudo-Goldstone boson.
- [17] J. A. Aguilar-Saavedra, Phys. Lett. B **625** (2005) 234 [Erratum-ibid. B **633** (2006) 792] [arXiv:hep-ph/0506187]; PoS **TOP2006** (2006) 003 [arXiv:hep-ph/0603199].

- [18] M. Carena, A. D. Medina, B. Panes, N. R. Shah and C. E. M. Wagner, arXiv:0712.0095 [hep-ph].
- [19] G. Azuelos *et al.*, Eur. Phys. J. C **39S2** (2005) 13 [arXiv:hep-ph/0402037]; D. Costanzo, ATL-PHYS-2004-004.
- [20] C. Dennis, M. Karagoz Unel, G. Servant and J. Tseng, arXiv:hep-ph/0701158.
- [21] W. Skiba and D. Tucker-Smith, Phys. Rev. D **75**, 115010 (2007) [arXiv:hep-ph/0701247].
- [22] ATLAS Detector and Physics Performance: Technical Design Report, Volume 2, CERN-LHCC-99-015, May 1999; Section 18.2.2.
- [23] R. Contino, T. Kramer, M. Son and R. Sundrum, JHEP **0705** (2007) 074 [arXiv:hep-ph/0612180].
- [24] R. Barbieri, B. Bellazzini, V. S. Rychkov and A. Varagnolo, arXiv:0706.0432 [hep-ph].
- [25] T. Aaltonen *et al.* [CDF Collaboration], Phys. Rev. D **76**, 072006 (2007) [arXiv:0706.3264 [hep-ex]]. See also: P. Q. Hung and M. Sher, arXiv:0711.4353 [hep-ph].
- [26] A. Abulencia *et al.* [CDF Collaboration], Phys. Rev. Lett. **98**, 221803 (2007) [arXiv:hep-ex/0702051].
- [27] J. Alwall *et al.*, JHEP **0709** (2007) 028 [arXiv:0706.2334 [hep-ph]]; F. Maltoni and T. Stelzer, JHEP **0302** (2003) 027 [arXiv:hep-ph/0208156]; T. Stelzer and W. F. Long, Comput. Phys. Commun. **81** (1994) 357 [arXiv:hep-ph/9401258].
- [28] T. Sjostrand, S. Mrenna and P. Skands, JHEP **0605** (2006) 026 [arXiv:hep-ph/0603175].
- [29] M.L. Mangano, presentation at the 2nd meeting of the ME/MC tuning working group, FNAL, Nov 15 2002, <http://cepa.fnal.gov/psm/MCTuning//15nov2002.html>; J. Alwall *et al.*, arXiv:0706.2569 [hep-ph]; M. L. Mangano, M. Moretti, F. Piccinini and M. Treccani, JHEP **0701** (2007) 013 [arXiv:hep-ph/0611129].
- [30] See <http://madgraph.phys.ucl.ac.be/>.
- [31] R. Bonciani, S. Catani, M. L. Mangano and P. Nason, Nucl. Phys. B **529**, 424 (1998) [arXiv:hep-ph/9801375].
- [32] F. Maltoni, D. L. Rainwater and S. Willenbrock, Phys. Rev. D **66**, 034022 (2002) [arXiv:hep-ph/0202205].
- [33] CMS physics: Technical Design Report, Volume I: Detector Performance and Software, CERN-LHCC-2006-001, February 2006; Section 9.1.
- [34] ATLAS Detector and Physics Performance: Technical Design Report, Volume 1, CERN-LHCC-99-014, May 1999; Section 3.3.

- [35] J. M. Butterworth, B. E. Cox and J. R. Forshaw, Phys. Rev. D **65** (2002) 096014 [arXiv:hep-ph/0201098].
- [36] B. Holdom, JHEP **0703**, 063 (2007) [arXiv:hep-ph/0702037].
- [37] J. M. Butterworth, J. R. Ellis and A. R. Raklev, JHEP **0705** (2007) 033 [arXiv:hep-ph/0702150].
- [38] U. Baur and L. H. Orr, Phys. Rev. D **76** (2007) 094012 [arXiv:0707.2066 [hep-ph]].
- [39] K. Agashe *et al.*, Phys. Rev. D **76** (2007) 115015 [arXiv:0709.0007 [hep-ph]].
- [40] S. Catani, Y. L. Dokshitzer, M. H. Seymour and B. R. Webber, Nucl. Phys. B **406** (1993) 187.
- [41] B. Lillie, L. Randall and L. T. Wang, JHEP **0709** (2007) 074 [arXiv:hep-ph/0701166].
- [42] G. Brooijmans, in: Proceedings of the Workshop “Physics at TeV Colliders”, 11-29 June 2007, Les Houches (France), to appear.
- [43] See for example: W.-M.Yao et al. (Particle Data Group), J. Phys. G **33**, 1 (2006).